mixture at -23 °C. The residue in the tube was $B_3H_7{\cdot}P(CH_3)_3$ contaminated with a small amount of $BH_2Cl{\cdot}P(CH_3)_3$ (^{11}B NMR).

Reaction of $B_3H_7{\cdot}P(CH_3)_3$ with BCl_3. A solution containing 0.76 mmol of $B_3H_7{\cdot}P(CH_3)_3$ in about 2 mL of CH_2Cl_2 was treated with a 0.92-mmol sample of BCl_3 at -80 °C for 2 h. No change was observed (^{11}B NMR). The mixture was allowed to warm slowly to room temperature, and then the volatile components were removed by pumping. Small amounts of chlorodiboranes were found in the volatile components (IR). The solid residue was $B_3H_7{\cdot}P(CH_3)_3$, and no $B_3H_6Cl{\cdot}P(CH_3)_3$ was found (^{11}B NMR).

Formation of $B_3H_6Cl{\cdot}(CH_3)_2NH$, $B_3H_6Cl{\cdot}CH_3NH_2$, and $B_3H_6Cl{\cdot}NH_3$. The chlorotriborane(7) adducts of dimethylamine, methylamine, and ammonia were prepared by the same procedure that was employed for the preparation of $B_3H_6Cl{\cdot}N(CH_3)_3$. In a typical reaction, a 1.36-mmol sample of $B_3H_7{\cdot}N(CH_3)_2H$, prepared in a 22-mm-o.d. Pyrex tube, was treated with a 0.75-mmol sample of BCl_3 in 3 mL of CH_2Cl_2 at -80 °C for 10 min. The resulting clear colorless solution was then warmed to 0 °C for 10 min while being stirred. Fractionation of the volatile components from the reaction tube at 0 °C yielded 0.20 mmol of B_2H_6. The resulting white solid product mixture contained $B_3H_6Cl{\cdot}(CH_3)_2NH$ (ca. 90%, ^{11}B NMR).

Formation of $B_3H_6Cl{\cdot}S(CH_3)_2$. A 0.62-mmol sample of $B_3H_7{\cdot}S(CH_3)_2$ was mixed with a 0.34-mmol sample of BCl_3 and 3 mL of CH_2Cl_2 at -80 °C, and the solution was allowed to warm to 0 °C. Then, volatile components were removed by pumping. The clear colorless liquid residue consisted of $B_3H_6Cl{\cdot}S(CH_3)_2$ (ca. 80%), $B_3H_7{\cdot}S(CH_3)_2$, $BHCl_2{\cdot}S(CH_3)_2$, and a small amount of $BHCl_2{\cdot}THF$ (^{11}B NMR).

Reactions of $B_3H_7{\cdot}PH_3$. (a) With HCl. A sample of about 1 mmol of $B_3H_7{\cdot}PH_3$ was mixed with a 1.78-mmol sample of HCl in 2 mL of CH_2Cl_2 at -80 °C. After the solution was allowed to stand for 2 h at -80 °C, no hydrogen gas was found in the tube, and a 1.76-mmol quantity of HCl was recovered from the mixture.

(b) With BCl_3. A 1.2-mmol smple of $B_3H_7{\cdot}PH_3$ was mixed with a 1.24-mmol sample of BCl_3 in 2 mL of CH_2Cl_2. The mixture was kept at -23 °C for 15 min. The ^{11}B NMR spectrum of the solution at -23 °C showed that no reaction had occurred.

(c) With HCl/BCl_3. [Formation of $B_3H_6Cl{\cdot}PH_3$]. To the mixture of $B_3H_7{\cdot}PH_3$ and BCl_3 in (b) above was added a 2.45-mmol sample of HCl. As the mixture was allowed to warm to room temperature, 1.06 mmol of hydrogen gas was evolved. When the volatile components were removed from the reaction mixture at 0 °C, a clear liquid remained in the tube. The ^{11}B NMR spectrum of this liquid in CH_2Cl_2 is shown in Figure 4.

In a separate experiment, a 1.0-mmol sample of $B_3H_7{\cdot}PH_3$ was treated with a mixture of HCl (2.22 mmol) and a BCl_3 (1.97 mmol) in CH_2Cl_2 at -80 °C. A 0.22-mmol quantity of hydrogen gas was evolved within a period of 0.5 h, and after an additional 0.5 h, a total of 0.33 mmol of hydrogen gas was collected. Then, volatile components were pumped out at -80 °C. The ^{11}B NMR spectrum of the residue in CH_2Cl_2 showed that it was a mixture of $B_3H_6Cl{\cdot}PH_3$ and $B_3H_7{\cdot}PH_3$ in a molar ratio of approximately 2:3.

Acknowledgment. This work was supported by the U.S. Army Research Office.

Contribution from the Department of Chemistry, LaTrobe University, Bundoora, Victoria 3083, Australia, and Department of Chemical and Analytical Science, Deakin University, Geelong, Victoria 3217, Australia

Electrochemistry of Cyanocopper Thiomolybdates and Thiotungstates: Redox-Based Interconversion of Species

Michael Kony,[1a,b] Alan M. Bond,*[,1c] and Anthony G. Wedd*[,1a]

Received January 18, 1990

$[MoS_4]^{2-}$ and its 1:1 and 1:2 CuCN adducts $[(CN)CuS_2MoS_2]^{2-}$ and $[(CN)CuS_2MoS_2Cu(CN)]^{2-}$ each exhibit electrochemically reversible one-electron reductions in MeCN at fast scan rates (>500 mV s^{-1}). At lower scan rates, the reduced adduct species are unstable to dissociation of CuCN, leading to interconversion of the three anions. The tungsten analogues show similar properties.

Introduction

Rich structural chemistries have emerged from the interaction of the thiomolybdate ligand $[MoS_4]^{2-}$ with metal fragments.[2,3] Those involving iron and copper are well developed, interest being driven by the bioinorganic importance of FeMoS and CuMoS aggregates.

$[MoS_4]^{2-}$ forms 1:1 and 1:2 adducts with CuCN:[4]

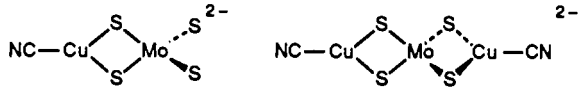

These anions are expected to be redox-active as a number of the related adducts formed with a variety of metal fragments undergo reduction processes.[5] While those reduced species can sometimes be trapped and studied,[5-7] they are invariably unstable on longer time scales and the nature of the subsequent chemical reactions is unknown.

Previous examination of $[MoS_4]^{2-}$ electrochemistry has shown complicated behavior (e.g. refs 8, 9). Conditions have been found in the present work for observation of a chemically and electrochemically reversible, one-electron reduction of $[MoS_4]^{2-}$ in MeCN. This has allowed a detailed examination of the electrochemistry of the CuCN adducts mentioned above and of their tungsten analogues. $[MoS_4]^{2-}$, $[(CN)CuS_2MoS_2]^{2-}$, and $[(CN)CuS_2MoS_2Cu(CN)]^{2-}$ each exhibit diffusion-controlled reversible one-electron reductions in MeCN at fast scan rates (>500 mV s^{-1}). However, at slower scan rates, the reduced adduct species are unstable to dissociation of CuCN, leading to interconversion of the three anions.

Experimental Section

Abbreviations and parameter symbols are given in ref 10.

(1) (a) La Trobe University. (b) Present address: Department of Chemistry, University of Tasmania, Hobart, Tasmania 7000, Australia. (c) Deakin University.
(2) Müller, A.; Diemann, E.; Jostes, R.; Bögge, H. *Angew. Chem., Int. Ed. Engl.* **1981**, *20*, 934.
(3) Garner, C. D. in *Comprehensive Coordination Chemistry* Wilkinson, G., Ed.; Pergamon: London, 1987; Vol. 3, p 1421.
(4) Gheller, S. F.; Hambley, T. W.; Rodgers, J. R.; Brownlee, R. T. C.; O'Connor, M. J.; Snow, M. R.; Wedd, A. G. *Inorg. Chem.* **1984**, *23*, 2519.
(5) Zanello, P. *Coord. Chem. Rev.* **1988**, *87*, 1.
(6) Bowmaker, G. A.; Boyd, P. D. W.; Campbell, G. K.; Zvagulis, M. *J. Chem. Soc., Dalton Trans.* **1986**, 1065.
(7) Coucouvanis, D.; Simtrou, E. D.; Stremple, P.; Ryan, M.; Swenson, D.; Baenziger, N. C.; Simopoulos, A.; Papaefthymiou, V.; Kostikas, A.; Petrouleas, V. *Inorg. Chem.* **1984**, *23*, 741.
(8) Pratt, D. E.; Laurie, S. H.; Dahm, R. H. *Inorg. Chim. Acta* **1987**, *135*, L21.
(9) You, J.; Wu, D.; Liu, H. *Polyhedron* **1986**, *5*, 535.
(10) Abbreviations: thf, tetrahydrofuran; SHE, standard hydrogen electrode; Fc^+/Fc, ferrocenium/ferrocene; $E_{1/2}^r$, reversible half-wave potential; E_p, peak potential; ΔE_p, peak-to-peak separation; v, scan rate; i_L, limiting current; i_p, peak current; i_{pr}, reduction peak current; i_{po}, oxidation peak current; ω, rotation frequency; n, electrons per molecule.

0020-1669/90/1329-4521$02.50/0

Table I. Redox Processes in MeCN Solutions (10^{-3} M in Redox-Active Species)

response[a]	couple	$E_{1/2}^r$, V[b]	n[b]
	$Fc^+ + e^- \rightleftharpoons Fc$	0.40	1.0
1, 1′	$[Mo^{VI}S_4]^{2-} + e^- \rightleftharpoons [Mo^{V}S_4]^{3-}$	−2.20	0.91
2, 2′	$[(CN)CuS_2Mo^{VI}S_2]^{2-} + e^- \rightleftharpoons [(CN)CuS_2Mo^{V}S_2]^{3-}$	−1.79	0.93
3, 3′	$[(CN)CuS_2Mo^{VI}S_2Cu(CN)]^{2-} + e^- \rightleftharpoons [(CN)CuS_2Mo^{V}S_2Cu(CN)]^{3-}$	−1.32	1.0
(4, 4′)[c]	$[(CN)CuS_2Mo^{V}S_2Cu(CN)]^{3-} + e^- \rightleftharpoons [(CN)CuS_2Mo^{IV}S_2Cu(CN)]^{4-}$	(−2.5)[c]	*c*
5, 5′	$[(CN)CuS_2Mo^{VI}OS]^{2-} + e^- \rightleftharpoons [(CN)CuS_2Mo^{V}OS]^{3-}$	−1.99	0.95
7, 7′	$[(CN)CuS_2W^{VI}S_2]^{2-} + e^- \rightleftharpoons [(CN)CuS_2W^{V}S_2]^{3-}$	−2.19	0.86
8, 8′	$[(CN)CuS_2W^{VI}S_2Cu(CN)]^{2-} + e^- \rightleftharpoons [(CN)CuS_2W^{V}S_2Cu(CN)]^{3-}$	−1.73	0.95

[a] Primes indicate oxidation processes observed on reverse scans of cyclic voltammograms. [b] Determined by rotating-disk voltammetry from the slope of plots of E versus ln $[(i_L - i)/i]$ and assuming the process to be electrochemically reversible. The n values are all concluded to be 1.0 after consideration of the limiting current data. [c] The redox process occurs close to the solvent limit, preventing quantitative analysis; E_{pc} is quoted.

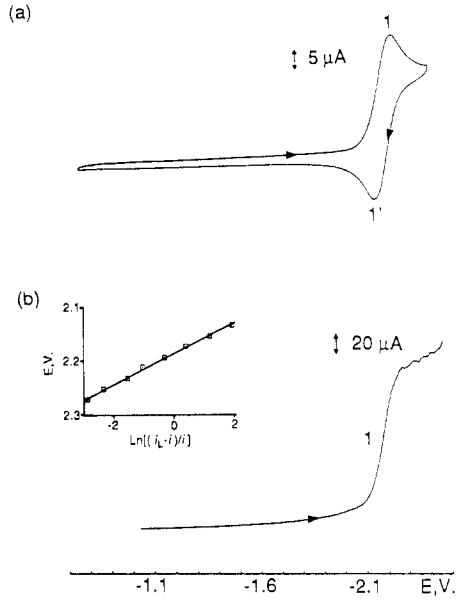

Figure 1. (a) Cyclic voltammogram of $[Et_4N]_2[MoS_4]$ (1.10 mM) in MeCN (v = 100 mV s^{-1}). (b) Rotating disk voltammogram of the same solution (v = 100 mV s^{-1}; ω = 157 s^{-1}). Inset: plot of E versus ln $[(i_L - i)/i]$.

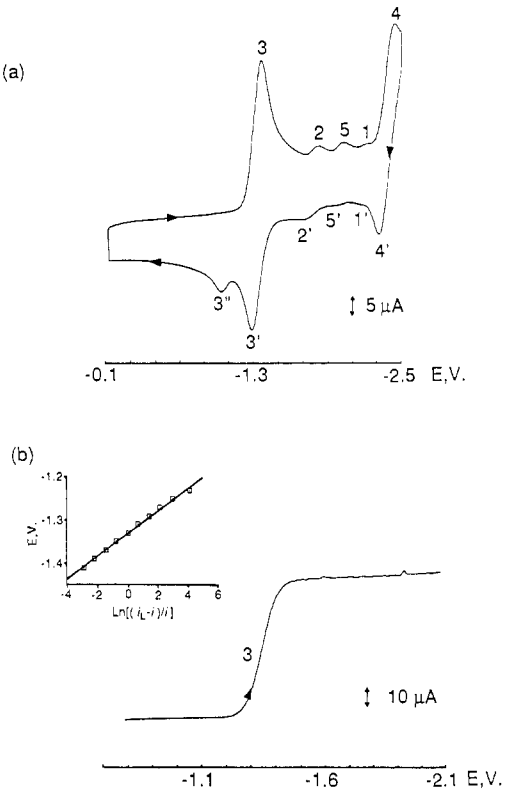

Figure 2. (a) Cyclic voltammogram of $[Pr^n_4N]_2[(CN)CuS_2MoS_2Cu(CN)]$ (1.00 mM) in MeCN (v = 200 mV s^{-1}). (b) Rotating disk voltammogram of the same solution (v = 100 mV s^{-1}; ω = 157 s^{-1}). Inset: plot of E versus ln $[(i_L - i)/i]$.

Synthesis of the salts $[Et_4N]_2[MS_4]$, $[Pr^n_4N]_2[(CN)CuS_2MS_2]$, $[Et_4N]_2[(CN)CuS_2MOS]$, and $[Pr^n_4N]_2[(CN)CuS_2MS_2Cu(CN)]$ (M = Mo, W) has been described previously.[4] MeCN and THF (May and Baker, analytical grade) were further purified as in refs 11 and 12. For electrochemistry, the solvents contained 0.2 M $Bu^n_4NBF_4$ as supporting electrolyte. Solvent-saturated dinitrogen was used to keep samples purged of dioxygen. Unless otherwise noted, data were obtained on solutions of concentration 1–2 mM at 22 ± 0.5 °C.

A BAS CV-27 voltammograph in conjunction with a Bausch & Lomb Houston series 100 recorder was used for cyclic voltammetry at a stationary electrode and for rotating-disk voltammetry. In each case, the working electrode was a Metrohm glassy-carbon disk of area 0.071 cm^2, and the auxiliary electrode was a platinum wire. The reference electrode was $Ag/AgNO_3$ (10^{-2} M) incorporated into a salt bridge containing supporting electrolyte to minimize Ag^+ contamination of the sample solution. It was calibrated repeatedly against the Fc^+/Fc couple. Reported $E_{1/2}^r$ values are referenced to the standard hydrogen electrode (SHE): for Fc^+/Fc, $E°$ = 0.400 V versus SHE.

The electrochemical cell was a Princeton Applied Research design (10 cm^3 volume) incorporating the above electrodes. The Fc^+/Fc couple is known[13] to satisfy the criteria for an electrochemically reversible, diffusion-controlled charge-transfer process (cyclic voltammetry: ΔE_p = 56 mV at 25 °C; $i_{po}v^{-1/2}$ independent of v). Due to an uncompensated iR drop in the cell, a range of values was observed in MeCN: ΔE_p = 60–79 mV and $i_{po}v^{-1/2}$ = 45–39 μA $s^{1/2}$ mM^{-1} cm^{-2} in the range v = 20–500 mV s^{-1} (Table S1). Analogous behavior for redox couples observed in this work was taken as evidence for electrochemical reversibility.[13b] Rotating disk voltammetry employed a Metrohm Model 628.10 unit. For Fc^+/Fc, i_L was proportional to $\omega^{1/2}$ (slope, 109 μA $s^{-1/2}$ mM^{-1} cm^{-2}; Table S2), indicating that the limiting current was diffusion-controlled.[14] A plot of E against ln $[(i_L - i)/i]$ was linear in slope close to the Nernstian value of RT/F and intercept $E_{1/2}^r$ at 0.40 V.

Results and Discussion

The electrochemistry of all thiometalate species examined exhibit oxidative processes at potentials more positive than −0.1 V vs SHE. As these processes induce formation of orange films on the working electrode that interfere with the electrode response, this study is restricted to those redox events occurring at potentials more negative than −0.15 V. The films appear to be a consequence of sulfide ligand oxidation but are not discussed further here.

$[Et_4N]_2[MS_4]$. In contrast to previous reports,[8,9] simple behavior is seen for reduction of $[MoS_4]^{2-}$ (Figure 1) provided the potential is kept more negative than −0.1 V and the negative solvent limit is avoided. The cyclic voltammetric data (Figure 1a; Table S3) indicate an electrochemically reversible couple (processes 1, 1′) in the range v = 20–1000 mV s^{-1}. Rotating disk voltammetry

(11) Perrin, D. D.; Armarego, W. L. F.; Perrin, D. R., Eds. *Purification of Laboratory Chemicals*; Pergamon Press: Oxford, U.K., 1980.
(12) Burfield, D. R.; Lee, K.-H.; Smithers, R. H. *J. Org. Chem.* **1977**, *42*, 3060.
(13) (a) Brown, E. R.; Lange, R. F. In *Techniques of Chemistry*; Weissberger, A., Rossiter, B. W., Eds.; Wiley: New York, 1971; Part 2A, Chapter 6. (b) Gagné, R. R.; Koval, C. A.; Lisensky, G. C. *Inorg. Chem.* **1980**, *19*, 2854.
(14) Bard, A. J.; Faulkner, L. R. *Electrochemical Methods*; Wiley: New York, 1980, Chapter 8.

(Figure 1b) shows that i_L is proportional to $\omega^{1/2}$ (Table S4) while a plot of E versus ln $[(i_L - i)/i]$ (Figure 1b) is linear with intercept $E_{1/2}^r = -2.20$ V and a slope similar to that for the known one-electron Fc^+/Fc value. The data are consistent with a chemically and electrochemically reversible, diffusion-controlled, one-electron couple (Table I):

$$[MoS_4]^{2-} + e^- \underset{1'}{\overset{1}{\rightleftharpoons}} [MoS_4]^{3-}$$

$[WS_4]^{2-}$ cannot be reduced within the available potential range in either MeCN or THF.

$[Pr^n_4N]_2[(CN)CuS_2MS_2Cu(CN)]$. Cyclic voltammetry in the range −0.1 to −2.5 V in MeCN detects five reduction processes (processes 3, 2, 5, 1, and 4) on the first reduction scan and six oxidation processes (processes 3″, 3′, 2′, 5′, 1′, and 4′) on the reverse scan (Figure 2) for M = Mo. Data as a function of scan rate and concentration (1–4 mM) are given in Table S5 for processes (3, 3′). At scan rates <500 mV s^{-1}, the current ratio $i_{po}i_{pr}^{-1}$ is less than 1, implying that chemical reactions follow the charge-transfer step. The current function $i_{pr}v^{-1/2}$ is essentially constant for [Mo] = 1–4 mM, suggesting that the rate-determining step for the chemical reaction(s) following charge transfer is of first order. The ΔE_p value at low scan rates is slightly less than that observed for Fc^+/Fc at equivalent concentrations, indicating that this term is also affected by kinetic effects from the following chemical reactions.

In cyclic voltammograms with $v > 500$ mV s^{-1}, processes (3, 3′) approach chemical and electrochemical reversibility and processes other than processes (4, 4′) are absent. Rotating-disk voltammetry detects reduction process 3 only (Figure 2b). Limiting current i_L is proportional to $\omega^{1/2}$ (Table S6) while a plot of E versus ln $[(i_L - i)/i]$ is linear (Figure 2b) providing $E_{1/2}^r = -1.32$ V while the slope indicates that $n = 1$. Consequently, process 3 is confirmed as a diffusion-controlled process in short time domains, and processes (3, 3′) are assigned to the one-electron couple (Table I)

$$[(CN)CuS_2MoS_2Cu(CN)]^{2-} + e^- \underset{3'}{\overset{3}{\rightleftharpoons}} [(CN)CuS_2MoS_2Cu(CN)]^{3-}$$

Processes (4, 4′) occur close to the solvent limit in MeCN (Figure 2a). It is more easily observed in THF, and a comparison of cyclic voltammetric current functions for processes 3 and 4 at fast scan rate (process 3, 18 ± 1; process 4, 18 ± 2 μA $s^{1/2}$ $mV^{-1/2}$) suggest that process 4 is also a one-electron reduction. It is plausibly assigned to the couple

$$[(CN)CuS_2MoS_2Cu(CN)]^{3-} + e^- \underset{4'}{\overset{4}{\rightleftharpoons}} [(CN)CuS_2MoS_2Cu(CN)]^{4-}$$

Of the other processes seen in Figure 2a, process 3″ occurs as a function of process 3 under conditions where the latter is chemically irreversible as do processes (1, 1′), which are due to the couple $[MoS_4]^{2-/3-}$ discussed above. Substantiation of this plus discussion of processes (2, 2′) and (5, 5′) are given below.

Cyclic voltammetric results for $[(CN)CuS_2WS_2Cu(CN)]^{2-}$ are qualitatively similar to those for the Mo analogue (Table S7), but a shift to more negative potentials of ca. 0.4 V permits observation of only the first two reduction processes (processes 8, 7) and two oxidation processes (processes 8, 8′) (Figure S1). For $v > 500$ mV s^{-1}, processes (8, 8′) approach electrochemical and chemical reversibility. Rotating-disk voltammetry detects reduction process 8 only. The limiting current i_L is proportional to $\omega^{1/2}$, and the linear plot of E against ln$[(i_L - i)/i]$ provides $E_{1/2}^r = -1.73$ V while the slope indicates that process 8 is a one-electron process. Consequently processes (8, 8′) are assigned to the one-electron couple

$$[(CN)CuS_2WS_2Cu(CN)]^{2-} + e^- \underset{8'}{\overset{8}{\rightleftharpoons}} [(CN)CuS_2WS_2Cu(CN)]^{3-}$$

Discussion of processes 7 and 8″ is taken up below.

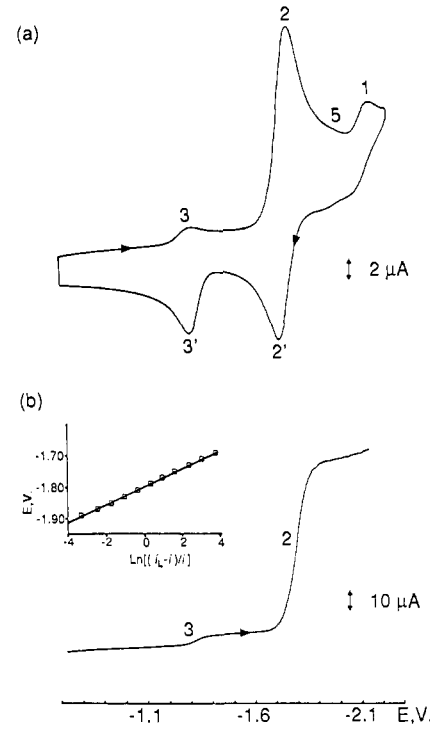

Figure 3. (a) Cyclic voltammogram of $[Pr^n_4N]_2[(CN)CuS_2MoS_2]$ (0.99 mM) in MeCN (v = 100 mV s^{-1}). (b) Rotating disk voltammogram of the same solution (v = 100 mV s^{-1}; ω = 314 s^{-1}). Inset: plot of E versus ln $[(i_L - i)/i]$.

$[Pr^n_4N]_2[(CN)CuS_2MS_2]$. Cyclic voltammetry for the Mo compound reveals four reduction processes (processes 3, 2, 5, and 1) on the first reduction scan and three oxidation processes (processes 3′, 2′, and 5′) on the reverse scan (Figure 3a). Data as a function of scan rate and concentration (1–4 mM) are given in Table S8 for processes (2, 2′). The observations closely parallel those of couple (3, 3′) of $[(CN)CuS_2MoS_2Cu(CN)]^{2-}$. In particular, at the faster scan rates and higher concentration, $i_{po}i_{pr}^{-1}$ approaches unity and ΔE_p has values similar to those observed for ferrocene. Consequently, for $v > 500$ V s^{-1}, couple (2, 2′) is chemically and electrochemically revesible in MeCN.

Rotating disk voltammetry detects reduction processes 3 and 2 (Figure 3b). Data for process 2 (Table S9) shows that i_L is proportional to $\omega^{1/2}$ and that a plot of E versus ln $[(i_L - i)/i]$ is linear (Figure 3b) providing $E_{1/2}^r = -1.79$ V and $n = 1$. Processes (2, 2′) are assigned to the one-electron couple (Table I)

$$[(CN)CuS_2MoS_2]^{2-} + e^- \underset{2'}{\overset{2}{\rightleftharpoons}} [(CN)CuS_2MoS_2]^{3-}$$

Of the other processes seen in Figure 3a, couple (3, 3′) due to $[(CN)CuS_2MoS_2Cu(CN)]^{2-/3-}$ always appears on the first scan in cyclic voltammetry and is also detected by rotating disk voltammetry (Figure 3b). This aspect is discussed further below. Reduction process 1 due to $[MoS_4]^{2-/3-}$ is not accompanied by oxidation process 1′, indicating that the reduced species $[MoS_4]^{3-}$ is scavenged on the time scale of the experiment. The sourceof couple (5, 5′) is discussed below.

Results for $[(CN)CuS_2WS_2]^{2-}$ are qualitatively similar to those for the Mo analogue, but peak potentials are shifted ca. −0.4 V (Figure S2, Table S10). Rotating-disk voltammetry provides estimates of $E_{1/2}^r = 2.19$ V and $n = 1$ for couple (7, 7′), the analogue of couple (2, 2′) (Table I).

$$[(CN)CuS_2WS_2]^{2-} + e \underset{7'}{\overset{7}{\rightleftharpoons}} [(CN)CuS_2WS_2]^{3-}$$

Couple (8, 8′) due to $[(CN)CuS_2WS_2Cu(CN)]^{2-/3-}$ is always seen on the first scan (Figure S2).

$[Et_4N]_2[(CN)CuS_2MOS]$. Cyclic voltammetry for the Mo compound reveals a prominant reduction (process 5) with the accompanying oxidation (process 5′) on the reverse scan (Figure S3). Data for processes (5, 5′) (Table S11) are similar to those

observed for $[(CN)CuS_2MS_2]^{2-/3-}$ (Tables S8 and S10). For $v > 500$ mV s^{-1}, processes (5, 5′) approach electrochemical reversibility. Under these conditions, rotating disk voltammetry provides estimates of $E_{1/2}^r = -1.99$ V and $n = 1$. Processes (5, 5′) are assigned to the couple

$$[(CN)CuS_2MoOS]^{2-} + e^- \underset{5'}{\overset{5}{\rightleftharpoons}} [(CN)CuS_2MoOS]^{3-}$$

Reduction processes for $[CN)CuS_2WOS]^{2-}$ occur close to the solvent limit. The only accurately definable parameter was $E_{pr} = -2.18$ V (v, 100 mVs^{-1}; [W], 1 mM).

Interconversion of Anions. Each of the anions examined exhibits a one-electron reduction (Table I) that approaches electrochemical and chemical reversibility at $v > 500$ mV s^{-1}. A change of W for Mo does not change the qualitative behavior, but analogous reversible half-wave potentials $E_{1/2}^r$ are shifted by about 0.4 V in the negative direction. As Mo^{VI} is generally observed to be more oxidizing than W^{VI}, the electron acceptor sites in these species can be assigned simplistically to the MS_4 sites. Similar observations obtain for $[(CO)_4MoS_2MS_2]^{2-}$, $[(CO)_4MoS_2MS_2Mo(CO)_4]^{2-}$, and $[(o\text{-xyl-}S_2)FeS_2MS_2]^{2-}$,[15,16] with direct EPR evidence being available for the latter system. The behavior contrasts with that of $[(S_5)FeS_2MS_2]^{2-}$ where replacement of W for Mo had little effect on peak potentials, suggesting that the Fe center functions as the electron acceptor site in that system.[17]

As Table I documents, reduction potentials become more positive in the order $[MS_4]^{2-}$, $[(CN)CuS_2MoS_2]^{2-}$, and $[(CN)CuS_2MS_2Cu(CN)]^{2-}$, consistent with a stabilization of the M-centered LUMO[18] due to overall electron donation to the CuCN fragments.

As shown above, processes (3, 3′) and (8, 8′), assigned to $[(CN)CuS_2MS_2Cu(CN)]^{2-/3-}$, always occur in solutions of $[(CN)CuS_2MS_2]^{2-}$ (Figures 3 and S2). When those processes only are scanned at $v = 500$ mV s^{-1} in such solutions, the current ratios $i_{po}i_{pr}^{-1}$ approach unity and the wave shapes assume the normal forms observed in solutions of $[(CN)CuS_2MS_2Cu(CN)]^{2-}$ (Figures 2 and S1). The observations are consistent with $[(CN)CuS_2MS_2Cu(CN)]^{2-}$ impurities being present in samples of $[(CN)CuS_2MS_2]^{2-}$ or with the presence of equilibrium 1.

$$2[(CN)CuS_2MS_2]^{2-} \overset{K_1}{\rightleftharpoons} [(CN)CuS_2MS_2Cu(CN)]^{2-} + [MS_4]^{2-} \quad (1)$$

The Mo systems were examined in more detail. Titration of $[MoS_4]^{2-}$ into a 1 mM solution of $[(CN)CuS_2MoS_2Cu(CN)]^{2-}$ causes the peak currents observed for processes 3 and 2 to respectively decrease and increase (Figure 4). That due to process 3 disappears after the addition of 1.5 equiv of $[MoS_4]^{2-}$ (Figure 4c). In addition, controlled-potential reductive electrolysis of solutions of $[(CN)CuS_2MoS_2]^{2-}$ at −1.45 V, slightly negative of process 3, does not eliminate that process as would be expected for the impurity $[(CN)CuS_2MoS_2Cu(CN)]^{2-}$ (vide infra). The observations favor the presence of equilibrium 1. The apparent equilibrium constant K_1 for Mo is calculated to be about 3×10^{-3} for Mo and even less for W based upon concentrations estimated from rotating disk voltammograms, assuming similar diffusion coefficients for 1:1 and 1:2 adducts (similar current functions can be noted in Tables S5, S8, and S10) and that the equilibrium is frozen on the voltammetric time scale. Given the small magnitude, it is not surprising that the relatively insensitive ^{95}Mo NMR failed to detect this equilibrium.[19]

There are three species involved in equilibrium 1 for M = Mo. Reversible half-wave potentials, $E_{1/2}^r$, for reduction of each can be calculated from rotating-disk voltammograms (Table I). Consequently a complete thermodynamic description of the one-electron reductive electron transfer processes associated with equilibrium 1 is available.

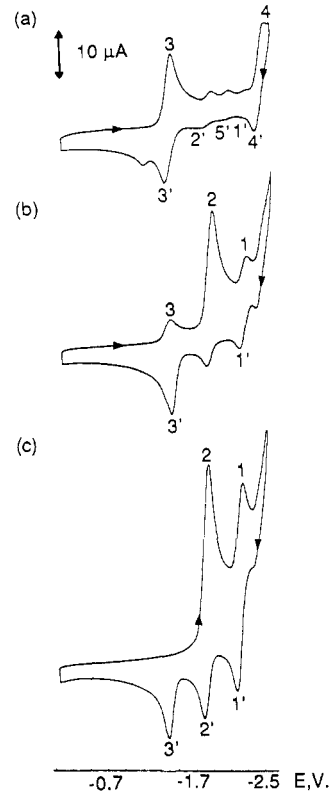

Figure 4. Cyclic voltammograms of $[Pr^n_4N]_2[(CN)CuS_2MoS_2Cu(CN)]$ (1.00 mM) in MeCN in the presence of $(Et_4N)_2[MoS_4]$ concentrations of (a) 0, (b) 0.75, and (c) 1.5 mM.

The next question to be addressed concerns the fate of products of reduction. At slow scan rates, multiple redox processes are observed (e.g., Figures 2a and 3a), and all can be positively assigned (Table I) except processes 3″ and 8″ (Figures 2 and S1), which arise as a result of reduction of $[(CN)CuS_2MS_2Cu(CN)]^{2-}$. The assignments are confirmed by current enhancement upon addition of the appropriate bona fide species. Consequently, data at slow scan rates are interpreted simply on the basis that dissociation and hydrolysis reactions occur upon reduction:

$$[(CN)CuS_2MS_2Cu(CN)]^{3-} \rightarrow [(CN)CuS_2MS_2]^{3-} + CuCN \quad (2)$$

$$[(CN)CuS_2MS_2]^{3-} \rightarrow [MS_4]^{3-} + CuCN \quad (3)$$

$$[(CN)CuS_2MS_2]^{3-} + H_2O \rightarrow [(CN)CuS_2MOS]^{3-} + H_2S \quad (4)$$

The reduced dissociation and hydrolysis products appear at potentials at which they are spontaneously oxidized (see $E_{1/2}^r$ values in Table I). The oxidized products are then detected voltammetrically when their reduction potentials are reached. Adventitious H_2O contained in solvent or electrolyte is apparently involved in reaction 4. Processes 3″ (Figure 2) and 8″ (Figure S1) may arise from the formation of a 1:3 adduct.[20]

The results demonstrate the reduction of $[(CN)CuS_2MoS_2(CN)]^{2-}$ and $[(CN)CuS_2MoS_2]^{2-}$ leads to dissociation of CuCN, giving access to thermodynamically allowed pathways that interconvert the tri-, bi-, and mononuclear anions in an interesting way. The scan rate dependence of the voltammetry is consistent

(15) Rosenhein, L. D.; McDonald, J. W. *Inorg. Chem.* **1987**, *26*, 3414.
(16) Friesen, G. D.; McDonald, J. W.; Newton, W. E. *Inorg. Chim. Acta* **1982**, *67*, L1.
(17) Coucouvanis, D.; Stremple, P.; Simhon, E. D.; Swenson, D.; Baenziger, N. C.; Draganjac, M.; Chan, L. T.; Simopoulos, A.; Papaefthymiou, V.; Kostikas, A.; Petrouleas, V. *Inorg. Chem.* **1983**, *22*, 293.
(18) Bernholc, J.; Stiefel, E. I. *Inorg. Chem.* **1985**, *24*, 1323.
(19) Minelli, M.; Enemark, J. H.; Brownlee, R. T. C.; O'Connor, M. J.; Wedd, A. G. *Coord. Chem. Rev.* **1985**, *68*, 169 (see p 197).

(20) Processes 3″ and 8″ appear at the potentials expected for oxidation of a reduced 1:3 $[MS_4]^{2-}$:CuCN adduct formed via

$$[(CuCN)_2MS_4]^{2-} \xrightarrow{e^-} [(CuCN)_2MS_4]^{3-} \xrightarrow{CuCN} [(CuCN)_3MS_4]^{3-}$$

Similar 1:3 adducts are known: Minelli, M.; Enemark, J. H.; Nicholson, J. R.; Garner, C. D. *Inorg. Chem.* **1984**, *23*, 4384.

Scheme I. Redox Interconversions[a]

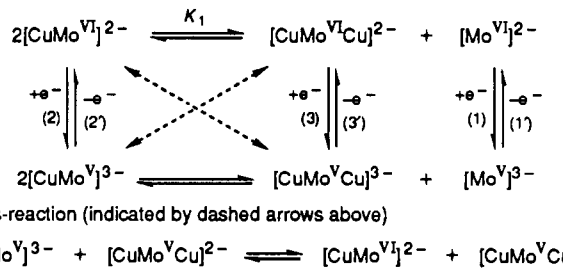

cross-reaction (indicated by dashed arrows above)

$$[CuMo^{V}]^{3-} + [CuMo^{V}Cu]^{2-} \rightleftharpoons [CuMo^{VI}]^{2-} + [CuMo^{V}Cu]^{3-}$$

[a] For simplicity the four sulfur atoms are omitted from each formula.

with the proposed chemical reactions 2–4 being coupled to the reduction processes listed in Table I.

Detailed interpretation is complicated by the presence of equilibrium 1 and the influence of redox cross-reactions. For example, the wave shapes observed for couple (3, 3′) in Figure 3 strongly suggest the presence of such processes. Although the present data at slow scan rates (where the kinetic effects of the following chemical reactions are observed) do not allow quantitative mechanistic interpretation of these effects, it does provide a qualitative indication of the nature of the following chemical reactions. The complexity of the system is illustrated by Scheme I, which details the possible redox interconversions, including cross-reactions.

On the other hand, the fast scan rate data provide a complete thermodynamic description for the six well-defined one-electron couples observed in the present system (Table I).

Acknowledgment. The Wool Research and Development Fund administered by the Australian Wool Corp. is thanked for financial support.

Supplementary Material Available: Figures S1–S3, showing cyclic voltammograms, and Tables S1–S11, listing cyclic voltammetry data for Fc^{+}/Fc, $[MoS_4]^{2-/3-}$ (1, 1′), $[(CN)CuS_2WS_2Cu(CN)]^{2-/3-}$ (3, 3′ and 8, 8′), and $[(CN)CuS_2MS_2]^{2-/3-}$ (2, 2′ and 7, 7′) and rotating disk electrode voltammetry data (i_L versus $\omega^{1/2}$) for processes 1–3 (14 pages). Ordering information is given on any current masthead page.

Contribution from Chemistry Department I, University of Copenhagen, Universitetsparken 5, DK-2100 Copenhagen Ø, Denmark, and Research School of Chemistry, The Australian National University, G.P.O. Box 4, Canberra, ACT 2601, Australia

Oxidation of Chelated Amino Acids to Imine Derivatives with Thionyl Chloride

Anders Hammershøi,*[1a] Richard M. Hartshorn,*[1b] and Alan M. Sargeson*[1b]

Received December 27, 1989

Various (α-amino acidato)cobalt(III) complexes have been treated with $SOCl_2$ in DMF. Provided the amino acid side chain does not contain functionalities that react with $SOCl_2$, the complex undergoes a facile oxidation to give the related α-imino acidato complex. A mechanism is proposed for these reactions.

Introduction

A considerable body of literature now exists on the enhanced reactivity of coordinated molecules toward both inter- and intramolecular nucleophiles.[2,3] The activating effect has been attributed to the ability of the metal ions to polarize bonds in the ligand, thus making it more susceptible toward attack by nucleophiles. For instance, the hydrolysis of acetonitrile is enhanced $\geq 10^6$-fold on coordination to cobalt(III), rhodium(III), and iridium(III). Moreover, the effect extends to the reduction of coordinated nitriles, which has been achieved by BH_4^-,[5] while a similar reduction of the free nitrile requires a considerably more potent reducing agent such as $LiAlH_4$. Coordinated imines are similarly activated, so that the nitromethane anion rapidly adds to the 2-iminopropionato complex **1** to give chelated α-nitro-

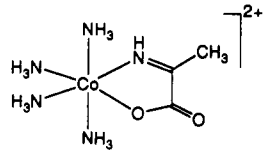

1

methylalanine.[4] It was considered for some time that this increased reactivity of coordinated ligands toward nucleophiles would be accompanied by a corresponding decrease in reactivity toward electrophiles. For this reason much effort has been spent investigating the reactions of coordinated ligands with nucleophiles, while not much has been done on reactions with highly electrophilic reagents, despite the fact that the metal ions may be employed to protect some sites and activate others in a ligand. Work using the Vilsmeier–Haack adduct derived from $POCl_3$ and DMF indicates that the metal ion can influence such electrophilic reactions in a useful way,[6–8] and presumably other electrophiles would also

Scheme I

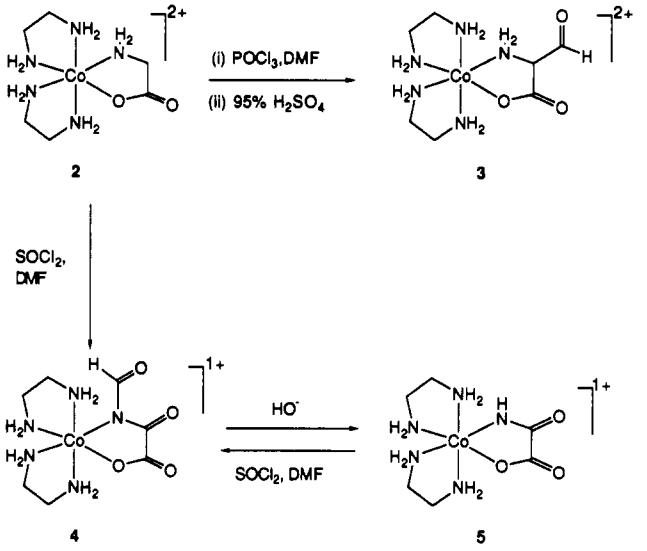

2 **3** **4** **5**

(1) (a) University of Copenhagen. (b) The Australian National University.
(2) Dixon, N. E.; Sargeson, A. M. In *Zinc Enzymes*; Spiro, T. G., Ed.; Wiley: New York, 1983: p 253.
(3) *Comprehensive Coordination Chemistry*; Wilkinson, G., Ed.; Pergamon: New York, 1987; Vol. I, Chapter 7.4, and Vol. VI, Chapters 61.1 and 61.4.
(4) Harrowfield, J. M.; Sargeson, A. M. *J. Am. Chem. Soc.* **1979**, *101*, 1514.
(5) Creaser, I. I.; Sargeson, A. M. *J. Chem. Soc., Chem. Commun.* **1975**, 974 and references therein.
(6) Jackson, W. G.; Sargeson, A. M.; Tucker, P. A.; Watson, A. D. *J. Am. Chem. Soc.* **1981**, *103*, 533.

0020-1669/90/1329-4525$02.50/0